Proton-Proton Weak Capture in Chiral Effective Field Theory

L. E. Marcucci, R. Schiavilla, and M. Viviani

Phys. Rev. Lett. **110**, 192503 — Published 10 May 2013

DOI: 10.1103/PhysRevLett.110.192503

The proton-proton weak capture in chiral effective field theory

L.E. Marcucci [a,b], R. Schiavilla [c,d], and M. Viviani [b]
[a] *Department of Physics, University of Pisa, 56127 Pisa, Italy*
[b] *INFN-Pisa, 56127 Pisa, Italy*
[c] *Department of Physics, Old Dominion University, Norfolk, VA 23529, USA*
[d] *Jefferson Lab, Newport News, VA 23606*

The astrophysical S-factor for proton-proton weak capture is calculated in chiral effective field theory over the center-of-mass relative-energy range 0–100 keV. The chiral two-nucleon potential derived up to next-to-next-to-next-to leading order is augmented by the full electromagnetic interaction including, beyond Coulomb, two-photon and vacuum-polarization corrections. The low-energy constants (LEC's) entering the weak current operators are fixed so as to reproduce the $A = 3$ binding energies and magnetic moments, and the Gamow-Teller matrix element in tritium β decay. Contributions from S and P partial waves in the incoming two-proton channel are retained. The S-factor at zero energy is found to be $S(0) = (4.030 \pm 0.006) \times 10^{-23}$ MeV fm^2, with a P-wave contribution of 0.020×10^{-23} MeV fm^2. The theoretical uncertainty is due to the fitting procedure of the LEC's and to the cutoff dependence.

PACS numbers: 25.10.+s, 26.20.Cd, 21.30.Fe

The proton weak capture on protons, *i.e.*, the reaction ^{1}H$(p, e^+\nu_e)^2$H (hereafter labelled pp), is the most fundamental process in stellar nucleosynthesis: it is the first reaction in the pp chain, which converts hydrogen into helium in main sequence stars like the Sun. Its reaction rate is expressed in terms of the astrophysical S-factor, $S(E)$, where E is the two-proton center-of-mass (c.m.) energy. At the center of light stars like the Sun, with temperature of the order of 1.5×10^7 K, the Gamow peak is at $E \simeq 6$ keV. At these energies, the reaction cross section cannot be measured in terrestrial laboratories, and it is necessary to rely on theoretical predictions, which are typically given for $S(0)$—the zero-energy value of the S-factor. The many studies on $S(0)$ have been extensively reviewed in Ref. [1], and are succinctly summarized next.

The currently recommended value for $S(0)$, $(4.01 \pm 0.01) \times 10^{-23}$ MeV fm^2 [1], is the average of values obtained within three different approaches, labelled "potential models" (PM), "hybrid chiral effective field theory" (χEFT*) and "pionless effective field theory" ($\not\pi$EFT). The first one uses phenomenological realistic models for the nuclear potential, fitted to reproduce the large body of two-nucleon (NN) bound and scattering state data with a χ^2/datum ~ 1. The axial current operator includes both one-body terms, determined from the coupling of the single nucleon to the weak probe, and two-body terms, derived from meson-exchange mechanisms and the excitation of Δ-isobar resonances. These two-body terms are constrained to reproduce the experimental value of the Gamow-Teller (GT) matrix element of tritium β-decay.

In the hybrid approach, transition operators derived in χEFT are sandwiched between initial and final wave functions generated by potential models. The only unknown low-energy constant (LEC), which parametrizes the strength of a contact-type four-nucleon coupling to the axial current, is determined by fitting the experimental GT matrix element.

Finally, $\not\pi$EFT is an effective field theory approach applicable to low-energy processes—such as the pp reaction under consideration here—with a characteristic momentum Q much smaller than the pion mass m_π. In such a theory, pions are integrated out and the NN interaction and weak currents are described by classes of point-like contact interactions, each class corresponding to given order in a systematic expansion in powers of Q/m_π.

The energy-dependence of $S(E)$ in the pp capture (and other reactions as well in the pp chain) is often parametrized as [1]

$$S(E) = S(0) + S'(0)E + S''(0)E^2/2 + \cdots \ , \qquad (1)$$

where $S'(0)$ and $S''(0)$ are the first and second derivatives of $S(E)$, evaluated at $E = 0$. For $S'(0)$ and $S''(0)$ the situation is much less clear than for $S(0)$. The adopted value for $S'(0)$ in Ref. [1] is $S'(0)/S(0) = (11.2 \pm 0.1)$ MeV^{-1}, as obtained in Ref. [2] and later confirmed in Ref. [3] in a PM approach. No value is reported for $S''(0)$ in Ref. [1]. In Ref. [2] it was estimated by dimensional considerations that the contribution of $S''(0)$ to the pp rate would be at the level of 1% for temperatures characteristic of the solar interior. Only very recently, $S'(0)$ and $S''(0)$ have been calculated in $\not\pi$EFT [4] to the third-order in the power expansion with the results $S'(0)/S(0) = (11.3 \pm 0.1)$ MeV^{-1} and $S''(0)/S(0) = (170 \pm 2)$ MeV^{-2}. In conclusion, a systematic study of $S(E)$ in (pionfull) χEFT is still missing. We address this omission in the present letter.

The NN potential is that derived in χEFT up to next-to-next-to-next-to leading order (N3LO) in the chiral expansion by Entem and Machleidt [5, 6]. However, in the

pp sector, it is augmented by the inclusion of higher-order electromagnetic terms, due to two-photon exchange and vacuum polarization. These higher-order terms are the same as those of the Argonne v_{18} (AV18) NN potential [7], and therefore also retain short-range corrections associated with the finite size of the proton charge distribution. The additional distortion of the pp wave function, induced primarily by vacuum polarization, has been shown to reduce $S(0)$ by $\sim 1\%$ in Ref. [3].

The charge-changing weak current has been derived up to N3LO in Ref. [8]. Its polar-vector part is related, via the conserved-vector-current constraint, to the (isovector) electromagnetic current, and includes, apart from one- and two-pion-exchange terms, two contact terms—one isoscalar and the other isovector—whose strengths are parametrized by the LEC's g_{4S} and g_{4V}. The two-body axial-vector current includes terms of one-pion range as well as a single contact current, whose strength is parametrized by the LEC d_R. The latter is related to the LEC c_D, which, together with c_E, enters the three-nucleon (NNN) potential at next-to-next-to leading order (N2LO), as illustrated in Fig. 1.

These chiral potentials and currents have power-law behavior in momentum space, and must be regularized before they can be used in practical calculations. This is accomplished by multiplying them by a momentum-cutoff function, whose cutoff Λ is taken to be in the range (500–600) MeV. Finally, we should note that inclusion of such a cutoff spoils the requirement of conserved-vector and partially-conserved-axial currents. In particular, we note that the construction of a conserved vector current with the N3LO NN potential used here would require accounting for two-loop corrections, a task well beyond the present state of the art.

The LEC's c_D (or d_R), c_E, g_{4S} and g_{4V} are determined with the procedure discussed in Ref. [9]. First, the values of the LEC's $\{c_D, c_E\}$ which reproduce the $A = 3$ binding energies are obtained for both $\Lambda = 500$ and 600 MeV, with c_D in the range $(-3, 3)$. Next, within this range, the GT matrix element is calculated and c_D (or equivalently d_R) is fixed to reproduce its experimental value. The range of c_D values, for which the calculated GT matrix element is within the lower and upper limits of its experimental determination, are $(-0.20, -0.04)$ for $\Lambda = 500$ MeV, and $(-0.32, -0.19)$ for $\Lambda = 600$ MeV. The corresponding ranges for c_E are $(-0.208, -0.184)$ and $(-0.857, -0.833)$, respectively [9]. Lastly, for the minimum and maximum values of $\{c_D, c_E\}$ and the given Λ, the isoscalar and isovector LEC's g_{4S} and g_{4V} are determined by reproducing the $A = 3$ magnetic moments. The values for all the LEC's are listed in Table I of Ref. [9]. Indeed, in that work it was shown that the consistent χEFT approach outlined above leads to predictions (with an estimated theory uncertainty of about 1%) for the rates of muon capture on deuteron and ^{3}He, that are in excellent agreement with the experimental data.

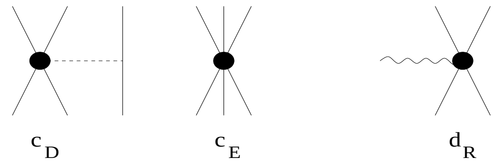

FIG. 1: One-pion exchange plus NN contact, and NNN contact terms entering the three-nucleon potential at N2LO, and the contact term entering the NN axial current. Solid, dashed, and wavy lines represent, respectively, the nucleon, pion, and external probe.

All earlier studies of the pp capture we are aware of (see Ref. [1] and references therein) have only considered the $^1S_0$ channel in the initial pp scattering state. Since one of the objectives of the present work is to study the energy dependence of the S-factor up to E=100 keV, we include, in addition to the $^1S_0$, the P-wave channels $^3P_0$, $^3P_1$, and $^3P_2$. We outline the calculation in the following, deferring a more extended discussion of it to a later paper [10].

The pp weak capture cross section $\sigma(E)$, from which the S-factor is obtained as $S(E) = E \exp(2\pi\,\eta)\,\sigma(E)$ ($\eta = \alpha/v_{\rm rel}$, α being the fine structure constant and $v_{\rm rel}$ the pp relative velocity), is written in the c.m. frame as

$$\sigma(E) = \int 2\pi\delta(\Delta m + E - \frac{q^2}{2m_d} - E_e - E_\nu)\frac{1}{v_{\rm rel}} \times\; F(Z, E_e)\frac{1}{4}\sum_{s_e\, s_\nu}\sum_{s_1\, s_2\, s_d} |\langle f|H_W|i\rangle|^2 \frac{d\mathbf{p}_e}{(2\pi)^3}\frac{d\mathbf{p}_\nu}{(2\pi)^3}\ , \quad (2)$$

where $\Delta m = 2\,m_p - m_d$ (m_p and m_d are the proton and deuteron masses, respectively), $\mathbf{p}_e$ ($\mathbf{p}_\nu$) and E_e (E_ν) are the electron (neutrino) momentum and energy, $\mathbf{q} = \mathbf{p}_e + \mathbf{p}_\nu$ is the momentum transfer, and $F(Z, E_e)$ is the Fermi function (with $Z = 1$), which accounts for the Coulomb distortion of the final positron wave function. Its explicit expression can be found in Ref. [11], increased by 1.62% to take into account radiative corrections to the cross section [12]. The transition amplitude is given by

$$\langle f|H_W|i\rangle = \frac{G_V}{\sqrt{2}} l^\sigma \langle -\mathbf{q}; d|j^\dagger_\sigma|\mathbf{p}; pp\rangle\ , \quad (3)$$

where G_V is the Fermi constant ($G_V = 1.14939 \times 10^{-5}$ GeV^{-2} [13]), $|-\mathbf{q}; d\rangle$ and $|\mathbf{p}; pp\rangle$ represent, respectively, the deuteron bound state with recoiling momentum $-\mathbf{q}$ and the pp scattering state with relative momentum $\mathbf{p}$, and l_σ and $j^\sigma(\mathbf{q})$ are the leptonic and nuclear weak currents, respectively. A standard multipole decomposition of the nuclear weak current operator leads to [14]

$$\frac{1}{4}\sum_{s_e\, s_\nu}\sum_{s_1\, s_2\, s_d} |\langle f|H_W|i\rangle|^2 = (2\pi)^2 G_V^2 L_{\sigma\tau} N^{\sigma\tau}\ , \quad (4)$$

where the lepton tensor $L^{\sigma\tau}$ is written in terms of electron and neutrino four velocities, and the nuclear tensor is defined as

$$N^{\sigma\tau} = \sum_{s_1\, s_2\, s_d} W^{\sigma}(\mathbf{q}; s_1 s_2 s_d)\, W^{\tau *}(\mathbf{q}; s_1 s_2 s_d) \ , \quad (5)$$

with

$$W^{\sigma=0,3}(\mathbf{q}; s_1 s_2 s_d) = \sum_{LSJ;\Lambda\geq 0} X_0^{LSJ\Lambda}(\hat{\mathbf{q}}; s_1 s_2 s_d) T_\Lambda^{LSJ}(q), (6)$$

$$W^{\sigma=\lambda}(\mathbf{q}; s_1 s_2 s_d) = -\frac{1}{\sqrt{2}} \sum_{LSJ;\Lambda\geq 1} X_{-\lambda}^{LSJ\Lambda}(\hat{\mathbf{q}}; s_1 s_2 s_d) \times \left[\lambda M_\Lambda^{LSJ}(q) + E_\Lambda^{LSJ}(q)\right] \ , \quad (7)$$

where $\lambda = \pm 1$ denote spherical components. The spin-quantization axis for the hadronic states is taken along the direction $\hat{\mathbf{p}}$ of the pp relative momentum. The functions $X_{\lambda=0,\pm 1}^{LSJ\Lambda}(\hat{\mathbf{q}}; s_1 s_2 s_d)$ depend on the direction $\hat{\mathbf{q}}$, the proton and deuteron spin projections s_1, s_2 and s_d, and we have used the notation $T_\Lambda^{LSJ}(q) = C_\Lambda^{LSJ}(q)$ or $L_\Lambda^{LSJ}(q)$ for $\sigma = 0$ or 3. The quantities $C_\Lambda^{LSJ}(q)$, $L_\Lambda^{LSJ}(q)$, $M_\Lambda^{LSJ}(q)$ and $E_\Lambda^{LSJ}(q)$ are, respectively, the reduced matrix elements (RME's) for the Coulomb, longitudinal, transverse magnetic and transverse electric multipole operators between the initial pp state with orbital angular momentum L, channel spin S ($S = 0, 1$), total angular momentum J, and the final deuteron state with total angular momentum $J_d = 1$. The number Λ in Eqs. (6) and (7) is the multipole order, with $\mathbf{\Lambda} + \mathbf{J} = \mathbf{J_d}$. The integrations over $\mathbf{p}_e$ and $\mathbf{p}_\nu$ are performed by Gaussian quadratures [14], and a moderate number of Gauss points ($\sim$ 10–20 for each integration) suffices to achieve convergence to within better than 1 part in 10^3.

The two-body wave functions corresponding to the non-local chiral potentials of Refs. [5, 6] have been obtained variationally with the technique described in Ref. [15]. In the present work, there is the complication due to the presence, in the pp sector, of higher-order corrections (from two-photon exchange and vacuum polarization) in the electromagnetic potential $v_{em}(r)$. We proceed in the following way. We first calculate the regular and irregular solutions corresponding to $v_{em}(r)$ only by direct integration of the the Schrödinger equation—these are denoted as $\Omega^{(R)}$ and $\Omega^{(I)}$. We then expand the pp continuum wave function in channel $\alpha \equiv LSJJ_z$ as

$$\Psi^\alpha = \sum_\mu c_\mu^\alpha \Psi_\mu^\alpha + \Omega_\alpha^{(R)} + \sum_{\alpha'} R_{\alpha\alpha'}\, \Omega_{\alpha'}^{(I)} \ , \quad (8)$$

where Ψ_μ^α are known functions written as product of Laguerre polynomials (see Eq. (3.1) of Ref. [15]), which vanish at large inter-particle separations. Clearly, the dependence on the NN potential enters only in the unknown coefficients c_μ and matrix elements $R_{\alpha\alpha'}$, which are determined via the Kohn variational principle. A system of linear inhomogeneous equations for the c_μ's and a set of algebraic equations for the $R_{\alpha\alpha'}$'s result, which are solved by standard techniques. From the $R_{\alpha\alpha'}$'s, phase shifts and mixing angles are easily obtained. We have verified that, in the case of the AV18, the method outlined above leads to $^1S_0$ phase shifts in agreement with those reported for the AV18 in Ref. [7] (which included the same $v_{em}(r)$ used here). We have also verified that we are able to reproduce the N3LO phase shifts of Ref. [6], obtained by including only the Coulomb potential in $v_{em}(r)$. Further details will be reported in a later publication [10].

The cumulative S- and P-wave contributions to the astrophysical S-factor at zero energy are listed in Table I. Inspection of the table shows that: (i) the cutoff dependence is negligible as is the overall theoretical uncertainty (well below 1%) due to the procedure adopted to fit the LEC's entering the current; (ii) the P-wave contributions to $S(0)$ sum up to $\sim$ 1% of the total value; (iii) the results can be summarized in the conservative range $S(0) = (4.030 \pm 0.006) \times 10^{-23}$ MeV fm^2. For comparison, we have also calculated $S(0)$ within the PM approach, using the AV18 potential and the same model for the nuclear current of Refs. [3, 14, 15], obtaining $S(0) = (4.033 \pm 0.003) \times 10^{-23}$ MeV fm^2 ($S(0) = (4.000 \pm 0.003) \times 10^{-23}$ MeV fm^2) when all the S- and P-waves (only the $^1S_0$ channel) are included. The agreement between the PM and χEFT results is excellent. Finally, it should be noted that the $^1S_0$ S-factor, in units of 10^{-23} MeV fm^2, obtained with the pure Coulomb interaction, is 4.025 when $\Lambda = 500$ MeV, and 4.030 within the PM approach with the AV18. Therefore, while the full electromagnetic interaction accounts for a $\sim$ 1% reduction in $S(0)$, this effect is in practice offset by the P-wave contributions.

TABLE I: Cumulative S- and P-wave contributions to the astrophysical S-factor at zero c.m. energy in units of 10^{-23} MeV fm^2. The theoretical uncertainties are given in parentheses and are due to the fitting procedure adopted for the LEC's in the weak current. The results have been obtained with the two different cutoff values $\Lambda = 500$ and 600 MeV.

	$^1S_0$	$^3P_0$	$^3P_1$	$^3P_2$
Λ=500 MeV	4.008(5)	4.011(5)	4.020(5)	4.030(5)
Λ=600 MeV	4.008(5)	4.010(5)	4.019(5)	4.029(5)

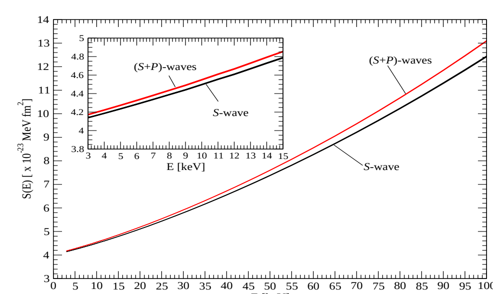

FIG. 2: (Color online) The astrophysical S-factor as function of the c.m. energy in the range 0–100 keV. The S- and $(S + P)$-wave contributions are displayed separately. In the inset, $S(E)$ is shown in the range 3–15 keV.

The energy dependence of $S(E)$ is shown in Fig. 2. The S- and $(S+P)$-wave contributions are displayed separately, and the theoretical uncertainty is included—the curves are in fact very narrow bands. As expected, the P-wave contributions become significant at higher values of E.

TABLE II: Values for $S^n(0)/S(0)$ with n = 1–4, in units of MeV^{-n}, and the χ^2 as defined in the text, obtained with a polynomial fit of $S(E)$ up to orders $O(E^2)$ (Fit 1), $O(E^3)$ (Fit 2), and $O(E^4)$ (Fit 3), retaining all $(S+P)$-waves. The results obtained by retaining only the S channel are listed separately for Fit 1 and 2. Also listed are the results of Ref. [4]. The theoretical uncertainties, listed only for $n = 1, 2, 3$, are given in parentheses and account for the cutoff sensitivity and the errors due to the LEC's fitting procedure.

n	1	2	3	4	χ^2
Fit 1	12.59(1)	199.3(1)			8.8×10^{-4}
Fit 2	11.94(1)	248.8(2)	–1183(8)		1.9×10^{-4}
Fit 3	11.34(1)	327.1(5)	–5592(12)	99 ×10^3	2.0×10^{-5}
S - Fit 1	12.23(1)	178.4(3)			1.2×10^{-3}
S - Fit 2	11.42(1)	239.6(5)	–1464(5)		1.9×10^{-4}
S - Ref. [4]	11.3(1)	170(2)			4.7×10^{-1}

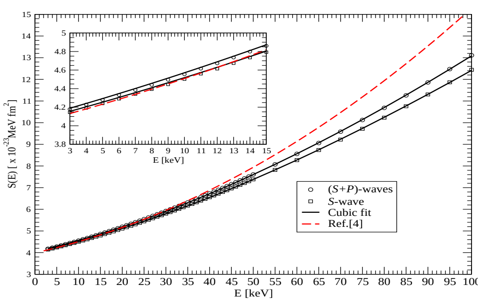

FIG. 3: (Color online) The astrophysical S-factor in the energy range 0–100 keV, calculated with Λ = 500 MeV and $c_D = -0.20$ and including the S- and $(S+P)$-wave contributions is compared with the cubic polynomial fit and the quadratic fit of Ref. [4]. In the inset, $S(E)$ is shown in the range 3–15 keV.

Next, we examine the question of whether the polynomial approximation for $S(E)$ given in Eq. (1) is justified. To this end, we have performed a least-squares polynomial fit to $S(E)$ up to order $O(E^2)$, *i.e.*, by using Eq. (1) itself, and up to order $O(E^n)$, by adding terms $S^n(0)E^n/n!$, with $n = 3, 4$ ($S^n(0)$ is the n-th derivative of $S(E)$ evaluated at $E = 0$). The values for $S^n(0)$, with n = 1–4, are listed in Table II, along with the χ^2 value, which we define as the sum over all the energy grid values of the "normalized" residuals, $\chi^2 = \sum_i (1 - f_i^{fit}/f_i^{calc})^2$, where f_i^{calc} (f_i^{fit}) are the calculated (fitted) $S(E)$ results. By inspection of the table, we conclude that the values of $S^n(0)$ are strongly dependent on the order of the polynomial function. However, an accurate description of the data can be obtained with a desired degree of accuracy by increasing the number of polynomial terms. With a cubic fit, for instance, $\chi^2 \sim 10^{-4}$ indicates that the calculated $S(E)$ values are nicely reproduced. This can be appreciated also in Fig. 3, where the cubic fit is compared with the results for $S(E)$ obtained retaining all $(S+P)$-waves or only the ${}^1S_0$ channel, using $\Lambda = 500$ MeV with one particular value of c_D ($c_D = -0.20$). The curve obtained using Eq. (1) with the values for $S(0)$, $S^{n=1}(0)$ and $S^{n=2}(0)$ of Ref. [4] is also shown. For energies up to 15 keV, the differences between our ${}^1S_0$ results and those of Ref. [4] are very small. However, at energies of 25–30 keV or higher, the quadratic fit of Ref. [4] starts to be significantly different from the calculated values, as well as from the cubic fit.

Finally, using the results corresponding to the cubic fit in Table II, we have calculated that the linear and quadratic contributions to $S(E)$ at the solar Gamow peak are of the order of 7% and 0.5%, respectively, while the cubic one is negligible. This is in agreement with Refs. [2, 4]. On the other hand, for larger-mass stars, whose central temperature is of the order of 5×10^7 K and the Gamow peak is at $E \sim 15$ keV, the linear, quadratic and cubic contributions become of the order of 18%, 3% and 0.7%, respectively.

The work of R.S. is supported by the U.S. Department of Energy, Office of Nuclear Science, under contract DE-AC05-06OR23177.

[1] E.G. Adelberger *et al.*, Rev. Mod. Phys. **83**, 195 (2011).
[2] J.N. Bahcall and R.M. May, Astrphys. J. **155**, 511 (1969).
[3] R. Schiavilla *et al.*, Phys. Rev. C **58**, 1263 (1998).
[4] J.-W. Chen, C.-P. Liu, and S.-H. Yu, arXiv:1209.2552
[5] D.R. Entem and R. Machleidt, Phys. Rev. C **68**, 041001 (2003).
[6] R. Machleidt and D.R. Entem, Phys. Rep. **503**, 1 (2011).
[7] R.B. Wiringa, V.G.J. Stoks, and R. Schiavilla, Phys. Rev. C **51**, 38 (1995).
[8] T.-S. Park, D.-P. Min, and M. Rho, Nucl. Phys. A **596**, 515 (1996); Y.-H. Song, R. Lazauskas, and T.-S. Park, Phys. Rev. C **79**, 064002 (2009); T.-S. Park *et al.*, Phys. Rev. C **67**, 055206 (2003).
[9] L.E. Marcucci, A. Kievsky, S. Rosati, R. Schiavilla, and M. Viviani, Phys. Rev. Lett. **108**, 052502 (2012).
[10] L.E. Marcucci, R. Schiavilla, M. Viviani, in preparation.
[11] G. Shen, L.E. Marcucci, J. Carlson, S. Gandolfi, and R. Schiavilla, Phys. Rev. C **86**, 035503 (2012).
[12] A. Kurylov, M.J. Ramsey-Musolf, and P. Vogel, Phys. Rev. C **67**, 035502 (2003).
[13] J.C. Hardy, I.S. Towner, V.T. Koslowsky, E. Hagberg, and H. Schmeing, Nucl. Phys. A **509**, 429 (1990).
[14] L.E. Marcucci, R. Schiavilla, M. Viviani, A. Kievsky, and S. Rosati, Phys. Rev. Lett. **84**, 5959 (2000); L.E. Marcucci *et al.*, Phys. Rev. C **63**, 015801 (2000).
[15] L.E. Marcucci *et al.*, Phys. Rev. C **83**, 014002 (2011).